On the Design of a Free Space Optical Link for Small Cell Backhaul Communication and Power Supply

On the Design of a Free Space Optical Link for Small Cell Backhaul Communication and Power Supply

John Fakidis*, Stepan Kucera†, Holger Claussen† and Harald Haas*

*Institute for Digital Communications
Li-Fi Research and Development Centre
The University of Edinburgh
Edinburgh, EH9 3JL, UK
Email: {j.fakidis, h.haas}@ed.ac.uk

†Bell Laboratories, Alcatel-Lucent
Blanchardstown Business & Technology Park
Dublin 15, Ireland
Email: {stepan.kucera,
holger.claussen}@alcatel-lucent.com

***Abstract*—The concept of small cells (SCs) is widely acknowledged for its significant benefits in energy efficiency and capacity of heterogeneous cellular networks. However, a large scale outdoor installation of SCs is limited by cost factors. Therefore, wireless backhaul communication and wireless power supply to SCs could significantly reduce deployment costs. The focus of this paper is on the investigation of the use of free space optical (FSO) links for power transfer to SCs in an indoor environment. In particular, an experimental design of a red light link for wireless power transmission (WPT) and energy harvesting (EH) is presented in the absence of ambient light. The transmitter includes up to five laser diodes (LDs) with a typical output optical power of 50 mW per LD. Light collimation is achieved by the use of aspheric lenses. The receiver comprises a crystalline silicon (c-Si) solar panel placed at 5.2 m from the optical transmitter. The use of five pairs of LDs and lenses results in a maximum harvested power of 10.4 mW. This study shows that the number of optical transmitters required for the generation of an electrical power of 1 W (demanded for the operation of a SC) from the solar panel is estimated to be 110.**

I. Introduction

The technology of small cells (SCs) is widely accepted as one of the most promising solutions to the exponential increase in capacity demand in wireless cellular networks [1]. Although a large scale outdoor deployment of SCs is beneficial in terms of network capacity and power consumption [2], the high cost represents the main restrictive factor. Wireless backhaul communication and alternative sources of power supply can make the installation of SCs more cost effective.

A potential power supply source for SCs is based on the concept of wireless power transmission (WPT). Wireless power transmission for long distance links is attainable only by radio frequency (RF) or microwave and laser-based systems [3]. In the RF region, receivers for energy harvesting (EH) are typically diode-based circuits termed 'rectennas' [4]. In the visible light (VL) spectrum, the widely available and low cost receivers for EH are solar panels. Every photovoltaic (PV) panel comprises a number of solar cells. In an outdoor scenario with SCs, a natural resource, i.e., sunlight, can significantly contribute to the harvested power in VL-based EH, whereas only 'dedicated' RF antennas can be used for RF-based WPT. However, the variability of weather conditions significantly affects the amount of harvested power. Therefore, the worst-case scenario of WPT from a 'dedicated' laser-based source or RF antenna is considered to be a complementary and reliable solution.

The emerging field of visible light communications (VLC) has been proposed as a complementary technology to RF systems, and as a candidate solution to the exponential increase in demand in wireless data transmission [5]. The great potential of VLC links created by off-the-shelf light-emitting diodes (LEDs) has been shown by the feasible transmission data rates of up to 3 Gb/s [6]. The capabilities of a solar panel receiver for both high speed data communication and EH were investigated in [7]. Therefore, the main objective of this research is the design of VLC or free space optical (FSO) links able to provide backhaul communication and power to SCs.

An optical wireless link formed by a high brightness white LED (WLED) and a parabolic mirror was investigated as a potential solution for SC EH in [8]. However, the amount of electrical power (18.3 mW) harvested from an amorphous silicon (a-Si) solar panel was too low for the required power of a SC of about 1 W. Also, the maximum link efficiency was significantly low (0.1%). This research is a follow-up study of [8]. This paper focuses on the aspects of exclusive laser-based WPT and solar panel-based EH at a distance of 5.2 m in an indoor environment. In particular here, a high power red light laser diode (LD) is used as an optical source. The selected wavelength of 660 nm allows for a visible and therefore practically uncomplicated alignment of the link components. Also, the spectral responsivity of typical crystalline silicon (c-Si) solar cells takes larger values close to the red region of the VL spectrum [9]. The use of two different lenses is examined for best light collimation. A multi-crystalline silicon (mc-Si) PV panel is used at the receiver. An analytical model of the system is presented for identifying the best lens and the optimum distance from the LD for efficient WPT. A set of two experimental studies is conducted. The number of optical transmitters, i.e., pairs of LD-lens, scales from one to five. An estimation of the required number of optical transmitters is made for the achievement of 1 W of electrical power harvested from the receiver. The main contribution of this paper is the

increase in the experimental maximum link efficiency by a significant factor of 7.4 for a $5.2\,\mathrm{m}$ link distance compared to the best result of our previous work [8].

The rest of the paper is organized as follows: Section II gives a physical system model. In Section III, the experimental set-up and studies are explained. In Section IV the results are summarized and discussed. Finally, Section V gives concluding remarks.

II. Analytical Model

The main components of the system implemented are LDs, lenses and a solar panel. The respective general analytical models for these are given in Sections II-A, II-B and II-C. Four important factors for the link efficiency are defined in Section II-D. The term 'far field' refers to the region further than the Rayleigh range introduced in Section II-A.

A. Single Laser Diode

In the far field, the relative optical intensity (or irradiance) versus the parallel and perpendicular to the junction angular divergence can be approximated by Gaussian curves of different widths [10]. Also, the selected LD operates at the fundamental transverse electrical (TE) mode. Therefore, an elliptical Gaussian beam propagation model is considered for the generated laser beam.

The Gaussian beam radii along the x- and y- direction are given by [11]:

$$W_{\mathrm{x}}(z) = W_{0\mathrm{x}}\sqrt{1+\left(\frac{z}{z_{0\mathrm{x}}}\right)^2}, \tag{1}$$

and:

$$W_{\mathrm{y}}(z) = W_{0\mathrm{y}}\sqrt{1+\left(\frac{z}{z_{0\mathrm{y}}}\right)^2}, \tag{2}$$

where $W_{0\mathrm{x}}$ is the beam waist radius along the x- axis; and $W_{0\mathrm{y}}$ is the beam waist radius along the y- axis. The values of $z_{0\mathrm{x}} = \pi W_{0\mathrm{x}}^2/\lambda_{\mathrm{p}}$ and $z_{0\mathrm{y}} = \pi W_{0\mathrm{y}}^2/\lambda_{\mathrm{p}}$ represent the Rayleigh range on the x- and y- axes, respectively. Quantity λ_{p} denotes the LD operating wavelength. At $z = z_{0\mathrm{x}}$ and $z = z_{0\mathrm{y}}$, the beam radius (or width) in the two transverse axes becomes $\sqrt{2}W_{0\mathrm{x}}$ and $\sqrt{2}W_{0\mathrm{y}}$, respectively. When $z \gg z_{0\mathrm{x}}$ and $z \gg z_{0\mathrm{y}}$, (1) and (2) can be transformed to:

$$W_{\mathrm{x}}(z) \simeq \frac{W_{0\mathrm{x}}}{z_{0\mathrm{x}}}z = \frac{\lambda_{\mathrm{p}}}{\pi W_{0\mathrm{x}}}z, \tag{3}$$

and:

$$W_{\mathrm{y}}(z) \simeq \frac{W_{0\mathrm{y}}}{z_{0\mathrm{y}}}z = \frac{\lambda_{\mathrm{p}}}{\pi W_{0\mathrm{y}}}z. \tag{4}$$

In the far field, the beam radii increase approximately linearly with z defining an elliptical cone of half angles:

$$\theta_{\mathrm{x}} = \tan^{-1}\left[\frac{W_{\mathrm{x}}(z)}{z}\right] \overset{(3)}{=} \tan^{-1}\left(\frac{\lambda_{\mathrm{p}}}{\pi W_{0\mathrm{x}}}\right), \tag{5}$$

and:

$$\theta_{\mathrm{y}} = \tan^{-1}\left[\frac{W_{\mathrm{y}}(z)}{z}\right] \overset{(4)}{=} \tan^{-1}\left(\frac{\lambda_{\mathrm{p}}}{\pi W_{0\mathrm{y}}}\right). \tag{6}$$

The defined half angles θ_{x} and θ_{y} are termed beam divergences in the x- and y- direction, respectively.

The q- parameters of the Gaussian beam in the x- and y- directions are described by [11]:

$$\frac{1}{q_{\mathrm{x}}(z)} = \frac{1}{R_{\mathrm{x}}(z)} - j\frac{\lambda_p}{\pi W_{\mathrm{x}}^2(z)}, \tag{7}$$

and:

$$\frac{1}{q_{\mathrm{y}}(z)} = \frac{1}{R_{\mathrm{y}}(z)} - j\frac{\lambda_p}{\pi W_{\mathrm{y}}^2(z)}, \tag{8}$$

where $R_{\mathrm{x}}(z)$ and $R_{\mathrm{y}}(z)$ denote the radii of curvature in the axes of the transverse plane. Radii of curvature are described by the relationships:

$$R_{\mathrm{x}}(z) = z\left[1+\left(\frac{z_{0\mathrm{x}}}{z}\right)^2\right], \tag{9}$$

and:

$$R_{\mathrm{y}}(z) = z\left[1+\left(\frac{z_{0\mathrm{y}}}{z}\right)^2\right]. \tag{10}$$

B. Free Space and Aspheric Lens

A convenient method to relate the input and output of an optical system is the use of ray transfer or $ABCD$ matrices [11]. The method of $ABCD$ matrices is also widely used in microwave communications [12]. In matrix optics, a simple 2×2 matrix connects the position and angle of paraxial rays at the input and output plane of an optical system through linear algebraic equations. Note that the application of $ABCD$ law to a Gaussian beam connects the q- parameters of the beam.

The $ABCD$ matrix of free space between the LD and the lens placed at a distance d_0 is:

$$\mathbf{M}_1 = \begin{bmatrix} 1 & d_0 \\ 0 & 1 \end{bmatrix}. \tag{11}$$

If a collimating lens is placed at its focal point as specified in the respective data sheet, the distance between the emission point of the source and input lens surface is termed back focal distance (BFD), and is given by [13]:

$$\beta = f\left[1-\frac{t_{\mathrm{c}}(n-1)}{nR_1}\right], \tag{12}$$

where quantity f denotes the effective focal length (EFL); t_{c} represents the thickness; and n is the refractive index of the lens material. Parameter R_1 denotes the radius of curvature of the input side of the lens.

The back surface of the aspheric lens is considered to be spherical. This assumption provides a worst-case scenario for the lens model. The elements of the $ABCD$ matrix for a thick lens, $\mathbf{M}_{\text{lens}}$, with two spherical surfaces of different radii of curvature are given below [13]:

$$A' = 1-\frac{t_{\mathrm{c}}(n-1)}{nR_1}, \tag{13}$$

$$B' = \frac{t_{\mathrm{c}}}{n}, \tag{14}$$

$$C' = -(n-1)\left(\frac{1}{R_1}-\frac{1}{R_2}\right) - \frac{t_{\mathrm{c}}(n-1)^2}{nR_1R_2}, \tag{15}$$

$$D' = 1+\frac{t_{\mathrm{c}}(n-1)}{nR_2}. \tag{16}$$

The value of R_2 denotes the radius of curvature of the output side of the lens.

Finally, the $ABCD$ matrix of free space between the output of the lens and the incidence plane to the solar panel is calculated by:

$$\mathbf{M}_2 = \begin{bmatrix} 1 & d-(d_0+t_c) \\ 0 & 1 \end{bmatrix}, \tag{17}$$

where d is the distance between the LD emission point and the solar panel. Therefore, the system $ABCD$ matrix can be written as the product of ray transfer matrices of individual components:

$$\mathbf{M} = \mathbf{M}_2\mathbf{M}_{\text{lens}}\mathbf{M}_1. \tag{18}$$

The general $ABCD$ matrix, $\mathbf{M}$, is applied to the elliptical Gaussian beam using the transformation [11]:

$$q_{\text{out}} = \frac{Aq_{\text{in}} + B}{Cq_{\text{in}} + D}, \tag{19}$$

where q_{in} and q_{out} denote the q- parameters of the Gaussian beam at the LD emission point ($z = 0$) and the input plane of the panel, respectively, either on the x- or y- axis.

C. Solar Panel

The selected solar panel consists of N_{C} cells connected in series. An effective single solar cell equivalent circuit for two or more cells connected in series is proposed in [14]. Also, a variable resistor, R_{L}, is connected to the output of the panel. A transcendental relationship between the load current, I_{L}, and voltage, V_{L}, describes the electrical behavior of the panel as given in [14]:

$$I_{0,\text{eff}}\left\{\exp\left[\frac{q}{A_{\text{eff}}k_{\text{B}}T}\left(V_{\text{L}} - R_{\text{S,eff}}I_{\text{L}}\right)\right] - 1\right\} + \\ + \frac{V_{\text{L}} - R_{\text{S,eff}}I_{\text{L}}}{R_{\text{P,eff}}} - I_{\text{Ph, eff}} - I_{\text{L}} = 0. \tag{20}$$

The physical constants $q = 1.602\times10^{-19}$ C and $k_{\text{B}} = 8.617\times10^{-5}$ eV/K represent the electron charge and Boltzmann constant, respectively. The temperature of the panel, T, is assumed to be 298 K. This model includes five unknown parameters, i.e., $I_{0,\text{eff}}$, $R_{\text{S,eff}}$, A_{eff}, $R_{\text{P,eff}}$ and $I_{\text{Ph,eff}}$. These parameters are strongly dependent on the values of optical power received from the panel. The value of $I_{0,\text{eff}}$ represents the effective dark saturation current of the diode. Parameters $R_{\text{S,eff}}$ and $R_{\text{P,eff}}$ denote the effective series and parallel resistance, respectively. The resistance R_{L} is considered to be part of $R_{\text{S,eff}}$. The size $I_{\text{Ph,eff}}$ is the effective generated photocurrent. The electrical power, P_{L}, harvested from the load resistor is given by $P_{\text{L}} = V_{\text{L}}I_{\text{L}}$. A simple 'exhaustive' search algorithm with discrete search space is implemented in order to estimate the five unknown parameters of the solar panel. The first part of (20) is the objective function of the problem, and is minimized. Then, the five identified parameters are applied to the model for curve fitting of the experimental data. The experimental measurements of I_{L} and V_{L} are used for finding a local solution to the non-linear curve-fitting problem.

TABLE I
FEATURES OF THE LASER DIODE

P_{typ} [mW]	λ_{p} [nm]	$\vartheta_{\parallel}$ [mrad]	$\vartheta_{\perp}$ [mrad]
50	660	174.5 (10°)	296.7 (17°)

D. Link Efficiency

An important aspect of the technology of WPT and EH is the total efficiency of a link. The external power efficiency of a LD can be defined as:

$$\eta_{\text{LD}} = \frac{P_{\text{Tx,o}}}{P_{\text{in}}} \times 100\%, \tag{21}$$

where $P_{\text{Tx,o}}$ denotes the output optical power of the LD and P_{in} is the direct current (DC) input electrical power. The fill factor (FF) of a solar panel shows how well the circuit approximates the ideal behaviour of a current source. The FF of a PV panel is given by [9]:

$$\text{FF} = \frac{V_{\text{m}}I_{\text{m}}}{V_{\text{oc}}I_{\text{sc}}} \times 100\%, \tag{22}$$

where V_{oc} and I_{sc} denote the open-circuit voltage and short-circuit current, respectively. Also, V_{m} and I_{m} represent the voltage and current at the maximum-power point (MPP) of the panel, respectively. The optical-to-electrical conversion efficiency or responsivity of the panel can be defined as:

$$\rho = \frac{I_{\text{Ph,eff}}}{P_{\text{Rx,o}}}, \tag{23}$$

where $P_{\text{Rx,o}}$ denotes the received optical power from the PV panel. Finally, the maximum link efficiency is computed by:

$$\eta_{\text{max}} = \frac{P_{\text{m}}}{P_{\text{in}}} \times 100\%, \tag{24}$$

where P_{m} denotes the maximum electrical power, and is given by: $P_{\text{m}} = V_{\text{m}}I_{\text{m}}$.

III. EXPERIMENTAL MODEL

Physical dimensions, and the electrical and optical characteristics of the components used are given in Section III-A. The objectives of each experimental study and the system set-up are explained in Section III-B.

A. System Components

A single mode Opnext HL6544FM high power LD with a multi-quantum well (MQW) structure is used as an optical source for WPT [10]. The semiconductor material of the LD is aluminium gallium indium phosphide (AlGaInP). Table I gives the data sheet values of the main features for this light source. Size P_{typ} denotes the typical value of output optical power. Angles $\vartheta_{\parallel}$ and $\vartheta_{\perp}$ refer to the full width at half maximum (FWHM) intensity in parallel and perpendicular plane to the junction, respectively.

The relatively large angular divergence of the optical source requires the use of a precise lens for light collimation. Although lenses with spherical surfaces are low cost and are relatively uncomplicated to manufacture, they have spherical aberrations [13]. This inherent defect of spherical lenses prevents

TABLE II
CHARACTERISTICS OF THE ASPHERIC LENSES

Part Number	R_1 [mm]	R_2 [mm]	t_c [mm]	f [mm]	r (%)
ACL12708U-A	15.65	−4.753	7.5	8.02	0.25
ACL4532	130	−18.281	18.5	32	10

efficient light collimation. In contrast, the complex geometry of aspheres allows for correction of spherical aberration and creates collimated beams of better quality [13]. Therefore, two aspheric condenser lenses are used in the experiments. The first condenser lens is an ACL12708U-A with anti-reflection (AR) coating and a diameter of 1.3 cm. The second lens is a 4.5 cm uncoated ACL4532. Table II gives the main features of both aspheres extracted from their respective data sheets [15], [16]. Quantities R_1, R_2, t_c and f have already been defined in Section II-B. The value of r (%) represents the reflectance of lens. The refractive index of the lens material is 1.52.

Finally, a SX 305 PV panel is used as the optical receiver for EH [17]. This solar panel comprises 36 mc-Si cells with silicon nitride (Si_3N_4) AR coating. The cells are placed in the form of a 4×9 matrix and are connected in series. The total effective area of the panel is $17.1 \times 22.8\,\text{cm}^2$. A maximum possible efficiency of 11.54% can be assumed from [17].

B. Experimental Studies

A series of two experimental studies is conducted in order to determine the maximum possible electrical power harvested from the solar panel. Load resistance is modified for the measurement of 21 pairs of (V_L, I_L) for every experimental scenario. Load voltage and current have values in the range of $[0, V_{oc}]$ and $[0, I_{sc}]$, respectively. The link distance is 5.2 m. Note that ambient light coming from the room luminaires contributes to the harvested power in the first study, and is ensured to be negligible in the second one.

1) Study I: Two experimental scenarios are implemented in the first study. A single pair of LD-lens is used in these scenarios. Also, the PV panel area is 'overfilled' with the red laser beam (the elliptical beam illuminates the total area of the rectangular panel and a small region around it). Note that the LD-lens distance (d_0) is set to be the optimum one to maximize the output power of the panel. The transmitter comprises the 4.5 cm lens placed at 2.6 cm from the LD in the first scenario. The second scenario is realized by the use of the 1.3 cm lens at 3.75 mm from the LD. An illustration of this scenario is given in Fig. 1(a).

2) Study II: This study consists of six different experimental scenarios. A lens with a diameter of 1.3 cm is used in all of these scenarios. From each of the first to fifth scenarios, the number of LD-lens pairs, N_{Tx}, scales from one to five, respectively. Laser diodes are connected in parallel. Distance d_0 for all of the LD-lens pairs is equal to 3.8 mm with a tolerance of ± 0.2 mm. Different laser beams 'overfill' the same total area of the panel. The fifth scenario implemented is shown in Fig. 1(b). The sixth scenario is realized by the use of five pairs of LD-lens. The only difference with the fifth scenario is that the optical transmitters point the laser beams at different regions of the solar panel. Therefore, different cells are illuminated by the five optical sources in this case.

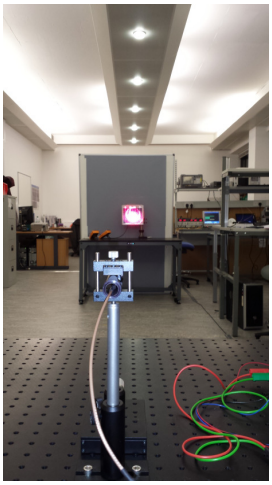

(a) Second scenario of Study I.

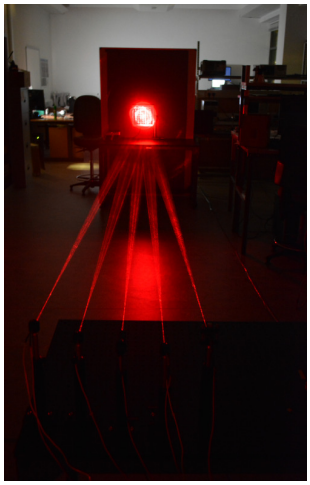

(b) Fifth scenario of Study II.

Fig. 1. Experimental red light laser links for WPT to a mc-Si-based panel at a distance of 5.2 m (a) with ambient light, and (b) without ambient light.

IV. RESULTS AND DISCUSSION

Essential parameters for the LD are calculated in Section IV-A. Analytical results are given in Section IV-B. The experimental results of the two studies are presented in Section IV-C. Finally, an estimation of the number of required LDs for harvesting 1 W of electrical power from the panel is presented in Section IV-D according to the physical model.

A. Calculation of the Laser Diode Parameters

In the far field pattern diagram from [10], the parallel and perpendicular to the junction beam divergences corresponding to the full width at 0^{th} intensity point are $2\theta_x = 40° = 698.13$ mrad and $2\theta_y = 80° = 1.4$ rad, respectively. The elliptical cone defined from these values of angular divergence contains 100% of the optical power. Solving (5) and (6) for W_{0x} and W_{0y}, respectively, results in: $W_{0x} = \lambda_p/[\pi \tan(\theta_x)] = 660/[\pi \tan(20°)] = 577.2$ nm, and $W_{0y} = \lambda_p/[\pi \tan(\theta_y)] = 660/[\pi \tan(40°)] = 250.37$ nm. Therefore, the rectangular cross section of the MQW laser source has the dimensions of $w = 2W_{0x} = 1.15$ µm, and $l = 2W_{0y} = 500.74$ nm $\simeq 0.5$ µm. The Rayleigh range in the x- and y- axis is calculated to be: $z_{0x} = \pi(577.2^2 \times 10^{-9})/660 = 1.586$ µm, and $z_{0y} = \pi(250.37^2 \times 10^{-9})/660 = 0.298$ µm, respectively. An output optical power $P_{Tx,o} = 62.6$ mW of the LD can be computed for a forward current of 120 mA from [10]. Therefore, for a DC input power $P_{in} = 282$ mW, the external power efficiency of the LD is $\eta_{LD} = 22.2\%$.

B. Analytical Results

An illustration of the Gaussian beam radii in the axes of x and y as a function of distance for five theoretical scenarios is shown in Fig. 2. These curves are derived using (3), (4) and (7)-(19). The system performance criterion is the collection of 100% of optical power from the solar panel.

Light collimation is improved in both axes by the addition of any of the two (1.3 cm or 4.5 cm) lenses compared to the non-collimated scenario (single LD). In the cases of setting the lenses at their focal points (pairs of orange and magenta

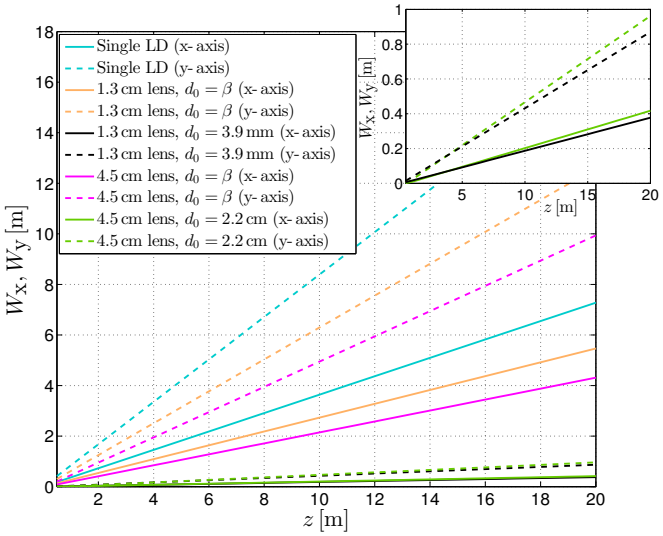

Fig. 2. Theoretical illustration of W_x, W_y [m] vs. z [m].

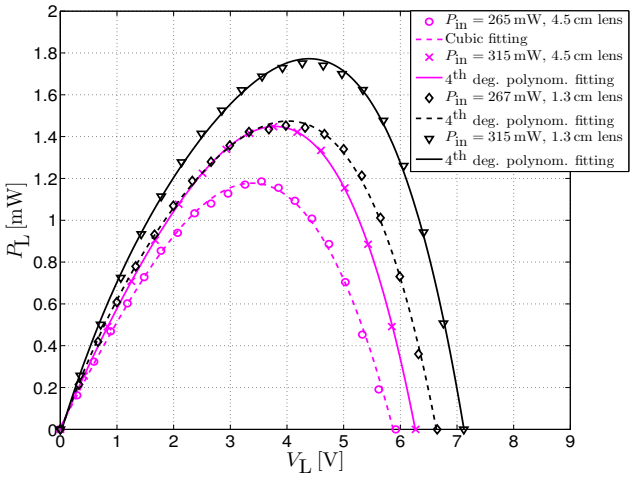

Fig. 3. Experimental V-P curves of Study I.

lines), the scenario of the 4.5 cm lens achieves better light transmission than that of the 1.3 cm one. This effect can be attributed to the longer radii of curvature of ACL4532 (see Table II) resulting in larger beam waists and Rayleigh ranges. A similar performance is attained for the lens-based scenarios (pairs of black and green lines), when the lenses are placed at the distances of 3.9 mm and 2.2 cm from the LD, respectively. Most importantly, it is observed that light collimation is further improved when either of the two aspheric lens is placed out of its focus and much closer to the LD. This is because the laser beam uses a smaller lens surface and the marginal rays are better collimated when focusing at larger distances. This theoretical effect indicates that in the experimental links the LD-lens distances should be set close to the theoretical values of 3.9 mm and 2.2 cm.

C. Experimental Results and Curve Fitting

The experimental data of (V_L, P_L) for Study I are shown in Fig. 3. Basic polynomial curve fitting is applied to each set of measurements. In terms of maximum harvested power, a gain factor of 1.2 is attained by the last scenario (black solid line) compared to the first one (magenta solid line) when the dissipated power at the transmitter is 315 mW. This finding is explained by the fact that the uncoated 4.5 cm lens attenuates the transmitted optical power to the solar panel more than the AR-coated 1.3 cm lens. This difference is also noticeable in the reflectance values of lenses, as presented in Table II.

The experimental results of Study II are given in Fig. 4. The curves labelled as 'physical model' are derived using (20). The values of FF and η_{max} measured for all of the six experimental scenarios are shown in Table III. Generally, the values of FF denote a low energy efficiency of the panel. This is attributed to both the low irradiance levels received as well as mismatch losses of the cells. As long as the irradiance distribution of the laser beam is elliptical and Gaussian, the cells placed at the edges of the PV panel are illuminated with lower optical power compared with the centrally-placed cells. Power generated by

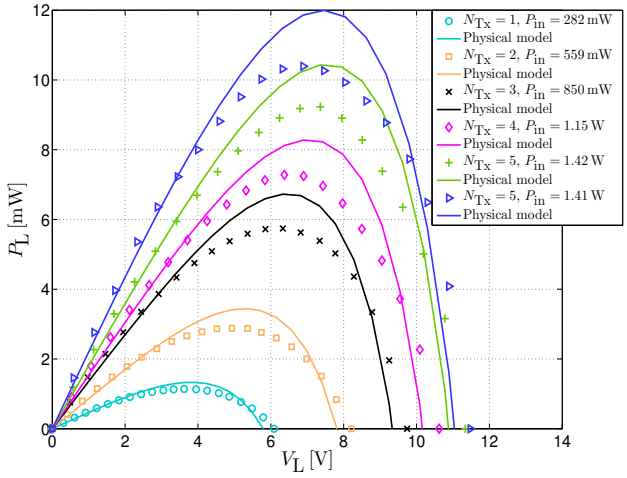

Fig. 4. Experimental V-P curves of Study II.

cells with higher illumination levels can be dissipated by cells with lower irradiance levels instead of the load. Therefore, the electrical output of the entire panel is determined by the cells with the lowest performance. The increase in η_{max} with the number of LDs used is due to a respective increase in the solar panel efficiency. However, this trend is not confirmed by scenarios 4 and 5. This can be explained by imperfections induced from the implementation of the optical transmitters. Although the best measured value of $\eta_{max} = 0.74\%$ is very low, note that the maximum possible is 2.56% for the components used ($22.2\% \times 11.54\% = 2.56\%$). This theoretical upper bound can be approximated by increasing N_{Tx}. The estimated values of the five solar panel unknown parameters for the six scenarios are given in Table IV. These five parameters scale with an increase in $P_{Rx,o}$ due to a respective increase in N_{Tx}, and this is in agreement with [18].

TABLE III
MEASURED FILL FACTOR AND MAXIMUM LINK EFFICIENCY

Scenario	1	2	3	4	5	6
FF (%)	34.4	34.7	37	39.3	38.7	36.2
$\eta_{\max}$ (%)	0.4	0.52	0.67	0.63	0.65	0.74

TABLE IV
ESTIMATED UNKNOWN PARAMETERS OF THE SOLAR PANEL

Scenario	$I_{0,\text{eff}}$ [μA]	$R_{\text{S,eff}}$ [Ω]	A_{eff}	$R_{\text{P,eff}}$ [kΩ]	$I_{\text{Ph, eff}}$ [mA]
1	117.3	1500	120	32	0.47
2	103.9	950	125	35.5	0.86
3	115.8	850	135	38	1.4
4	111.8	750	140	40.5	1.5
5	116.9	650	145	41.5	1.8
6	229.2	600	175	42	2.2

D. Estimation of the Number of Optical Transmitters

Let $N_{\text{Tx,req}}$ be the required number of pairs of LDs and lenses for $P_{\text{m}} = 1\,\text{W}$ at $d = 5.2\,\text{m}$. In scenario 6 (five optical transmitters), a value of $V_{\text{m}} = 6.89\,\text{V}$ is achieved with $P_{\text{m}} = 10.39\,\text{mW}$. Therefore, a maximum possible value of $V_{\text{m}} = 16.5\,\text{V}$ can be assumed for the solar panel at high illumination levels for attaining $P_{\text{m}} = 1\,\text{W}$ according to [17]. The load current at MPP is calculated to be $I_{\text{m}} = 1/16.5 = 60.6\,\text{mA}$. The values of $16.5\,\text{V}$ and $60.6\,\text{mA}$ are substituted for V_{L} and I_{L}, respectively, in (20). Then, the application of the 'exhaustive' search algorithm to (20) results in the following set of parameters: $(1.1\,\text{mA}, 0.1\,\Omega, 290, 90\,\text{k}\Omega, 69.1\,\text{mA})$. The responsivity of the solar panel is assumed to be $\rho = 0.01\,\text{mA/mW}$. Solving (23) for $P_{\text{Rx,o}}$ results in: $P_{\text{Rx,o}} = I_{\text{Ph,eff}}/\rho = 69.1/0.01 = 6.91\,\text{W}$. The total amount of optical power is considered to be received from the panel, i.e., $P_{\text{Rx,o}} = N_{\text{Tx,req}} P_{\text{Tx,o}}$. Therefore, the required number of optical transmitters is calculated to be: $N_{\text{Tx,req}} = P_{\text{Rx,o}}/P_{\text{Tx,o}} = 6.91/(62.6 \times 10^{-3}) \approx 110$.

V. SUMMARY AND CONCLUSIONS

The great potential of high speed data transmission for VLC systems has been extensively researched and demonstrated. However, the two-fold objective of simultaneous data communication and WPT in the optical domain remains an unexplored research area. Therefore, the capabilities of a red light laser-based link for WPT and EH from an off-the-shelf mc-Si solar panel were investigated in this study. In particular, the performance of two aspheric lenses was experimentally compared for best light collimation. Also, an analytical model was used to identify the optimum distance between light source and lens. A second experimental study was conducted using one to five pairs of LD and lens, i.e., optical transmitters, in an indoor environment in the absence of ambient light. The maximum link efficiency attained from five optical transmitters was $0.74\,\%$, and the respective maximum harvested power was $10.4\,\text{mW}$ for a link distance of $5.2\,\text{m}$. These values were too low for the required power of a SC of $1\,\text{W}$. This effect was explained by the low levels of optical power received and also mismatch losses among cells of the panel. An estimated number of 110 optical transmitters was required for harvesting $1\,\text{W}$ from the panel. While currently the overall link efficiency and harvested power are in the order of 1% and a few mW, respectively, the contribution of power from ambient light remains unexploited in this context. Future work will consider a larger number of LDs with higher power efficiency in order to increase the solar panel efficiency and the maximum link efficiency.

ACKNOWLEDGMENT

We acknowledge partial financial support by Bell Labs, Alcatel-Lucent Ireland. Professor Haas acknowledges support from the Engineering and Physical Sciences Research Council (EPSRC) under the Established Career Fellowship grant EP/K008757/1.

REFERENCES

[1] H. Claussen, L. T. Ho, and L. G. Samuel, "An Overview of the Femtocell Concept," *Bell Labs Tech. J.*, vol. 13, no. 1, pp. 221–245, 2008.

[2] R. Razavi and H. Claussen, "Urban Small Cell Deployments: Impact on the Network Energy Consumption," in *Proc. IEEE Wireless Commun. and Netw. Conf. Workshops (WCNCW)*, Paris, France, Apr. 1 2012, pp. 47–52.

[3] C. R. Valenta and G. D. Durgin, "Harvesting Wireless Power: Survey of Energy-Harvester Conversion Efficiency in Far-Field Wireless Power Transfer Systems," *IEEE Microw. Mag.*, vol. 15, no. 4, pp. 108–120, May 2014.

[4] U. Olgun, C.-C. Chen, and J. Volakis, "Investigation of Rectenna Array Configurations for Enhanced RF Power Harvesting," *IEEE Antennas Wireless Propag. Lett.*, vol. 10, pp. 262–265, Apr. 2011.

[5] H. Elgala, R. Mesleh, and H. Haas, "Indoor Optical Wireless Communication: Potential and State-of-the-Art," *IEEE Commun. Mag.*, vol. 49, no. 9, pp. 56–62, Sep. 2011.

[6] D. Tsonev, H. Chun, S. Rajbhandari, J. McKendry, S. Videv, E. Gu, M. Haji, S. Watson, A. Kelly, G. Faulkner, M. Dawson, H. Haas, and D. O'Brien, "A 3-Gb/s Single-LED OFDM-Based Wireless VLC Link Using a Gallium Nitride μLED," *IEEE Photon. Technol. Lett.*, vol. 26, no. 7, pp. 637–640, Apr. 2014.

[7] Z. Wang, D. Tsonev, S. Videv, and H. Haas, "On the Design of a Solar-Panel Receiver for Optical Wireless Communications with Simultaneous Energy Harvesting," *IEEE J. Sel. Areas Commun.*, vol. PP, no. 99, pp. 1–1, 2015.

[8] J. Fakidis, M. Ijaz, S. Kucera, H. Claussen, and H. Haas, "On the Design of an Optical Wireless Link for Small Cell Backhaul Communication and Energy Harvesting," in *Proc. IEEE 25th Int. Symp. Pers. Indoor and Mobile Radio Commun. (PIMRC)*, Washington, DC USA, Sep. 2–5 2014, pp. 32–36.

[9] A. Luque and S. Hegedus, Eds., *Handbook of Photovoltaic Science and Engineering*, 2nd ed. John Wiley & Sons, Mar. 2011.

[10] Opnext, "HL6544FM Visible High Power Laser Diodes," Retrieved May 19, 2014 from http://www.thorlabs.de/thorcat/21700/HL6544FM-MFGSpec.pdf, Mar. 2009.

[11] B. E. A. Saleh and M. C. Teich, *Fundamentals of Photonics*, 1st ed., ser. Wiley Series in Pure and Applied Optics. John Wiley & Sons, Inc., Jan. 1991.

[12] D. M. Pozar, *Microwave Engineering*, 4th ed., A. Melhorn, Ed. John Wiley & Sons, Dec. 2011.

[13] E. Hecht, *Optics*, 4th ed., A. Black, Ed. Addison-Wesley, 2002.

[14] A. Bauer, J. Hanisch, and E. Ahlswede, "An Effective Single Solar Cell Equivalent Circuit Model for Two or More Solar Cells Connected in Series," *IEEE J. Photovolt.*, vol. 4, no. 1, pp. 340–347, Jan. 2014.

[15] Thorlabs, "ACL12708U-A - Aspheric Condenser Lens, AR-Coated 350-700 nm, 1/2", f=8 mm," Retrieved May 22, 2014 from http://www.thorlabs.de/thorcat/CTN/ACL12708U-A-AutoCADPDF.pdf, Nov. 2013.

[16] ——, "ACL4532 - Aspheric Condenser Lens, 45 mm, f=32 mm, NA=0.612, Uncoated," Retrieved May 30, 2014 from http://www.thorlabs.de/thorcat/19000/ACL4532-AutoCADPDF.pdf, Sep. 2009.

[17] BP Solar, "BP Solar SX 305 5W PV Module," Retrieved June 4, 2014 from http://www.omniinstruments.co.uk/images/downloads/3353.pdf, Jul. 2007.

[18] A. Ortiz-Conde, D. Lugo-Munoz, and F. J. Garcia-Sanchez, "An Explicit Multiexponential Model as an Alternative to Traditional Solar Cell Models with Series and Shunt Resistances," *IEEE J. Photovolt.*, vol. 2, no. 3, pp. 261–268, Jul. 2012.